Journal of Robotics, Computer Vision and Graphics
Vol. 1, No. 1, 2016, pp. 12-20
http://www.aiscience.org/journal/jrcvg

Determining the Accuracy of Finite Element Analysis when Compared to Experimental Approach for Measuring Stress and Strain on a Connecting Rod Subjected to Variable Loads

Ikpe Aniekan Essienubong*, Owunna Ikechukwu, P. O. Ebunilo

Department of Mechanical Engineering, University of Benin, Benin City, Nigeria

Abstract

The basic idea of tensile testing plays a major role in determining how durable any member of a component will behave under the action of forces. This implies placing a material of known dimensions on the universal testing machine with one end fixed while extending the other end until the material breaks at a point with the highest stress and strain concentration and a tie rod of known dimensions was the material in this case. Also, similar approach was carried out using Finite Element Analysis (FEA). This paper encompasses experimental exercise where a connecting rod was subjected to tensile loading and the resultant stresses along the connecting rod due to strain which is a measure of the extent at which the connecting rod stretches (how much strain the connecting rod can undergo) when subjected to tensile loading. Three strain gauges were mounted on the con rod and were used in measuring the strains for varying load values through a digital meter. The results of the measured strains were compared to the strain predicted by FEA. While the material was under tension, it was observed that the material obeyed Hooks law which in this case implies that the load acting on the connecting rod was directly proportional to the extension since the connecting rod was not stretched until the elastic limit was exceeded. The results obtained from each procedure showed close relationship between the experimental exercise and FEA approach. This implies that FEA analysis is viable and can be used to prevent failure by predicting the severity of stress and strain concentration on a connecting rod before launched into operation and after operation. Experimental Procedures provided byVishay Precision Group (2010) was adopted as the experimental procedures for the strain measurement.

Keywords

Connecting Rod, Failure, Load,Safety, Simulation, Strain Gauge,Tensile Testing, Vibration

Received: May 18, 2016 / Accepted: May 28, 2016 / Published online: June 23, 2016

1. Introduction

Predicting the consequent loading effect on bodies with irregular shapes requires more complex procedures than it is needed for bodies like beams, rods, and so on. Resulting to physical observations alone cannot adequately evaluate the situation of such irregular bodies under such loads. Large deflections or elongations are visible but it is not the case for very small elongations or deflections. This is because such deflections can alter the natural frequency of vibrating bodies. Hence it is necessary to be able to determine or measure the small strains as well as large ones [8]. Determining either of stresses, deflections or strains is enough to help determine the state of a body under any load. With the discovery of the principle of operation of the strain gauge in 1856 by Lord Kelvin, component or structure stresses are determined by manufacturers of load cells, torque and pressure transducers and many more using the physical parameters measured in a linear way. It is worth mentioning

* Corresponding author
E-mail address: ikpeaniekan@gmail.com (I. A. Aniekan), ikechukwu.owunna@uniben.edu (O. Ikechukwu), Patrick.ebunilo@uniben.edu (P. O. Ebunilo)

that stress cannot be measured directly but strain can be, for many materials within their elastic limit [1]. The relationship between stress and strain which is a linear one for uniaxial loading conditions enables stress to be calculated easily. Both deflections and strains can either be measured or calculated and strain values may vary with the axis of measurement [4]. Elongations are dependent also on the axis of measurement and so is stress. Strains are measured by using strain gauges while most tensile testing equipment will indicate the values of axial deflection for uniaxial loading. It is of importance to state that strain measuring equipment use often times very small components that makes it rather often impossible to accurately position them on the strain axis of a test piece for measurement. Strain measurements are therefore often taken on different locations along the material under test.

2. Mathematical Method of Analysing Strain

Various kinds of mathematical models exist for evaluating strain for any system under load. The mathematical expressions are built around a general stress and strain relationship called hook's law. Lanza [10] defined Hooke's law as "stress is directly proportional to strain". This however is not true throughout the life cycle of a material. This is the essential reason why the study of strain is of necessity for every engineer. Hooke's law can therefore be defined as thus; "Within the elastic limit of a solid material, the deformation (strain) produced by a force (stress) of any kind is proportional to the force. If the elastic limit is not exceeded, the material returns to its original shape and size after the force is removed, other it remains deformed or stretched. The force at which the material exceeds its elastic limit is called limit of proportionality [2, 3, 13]. Generally, strain can be defined as the linear deformation of a component which is as result of application of force or load on the component. Figure 1 is a graphical representation of Hooke's law. The curve begins with a straight line curve which defines the elastic region of the material in question. In this region, stress and strain have a linear relationship and the slope of the curve is the young's modulus of elasticity.

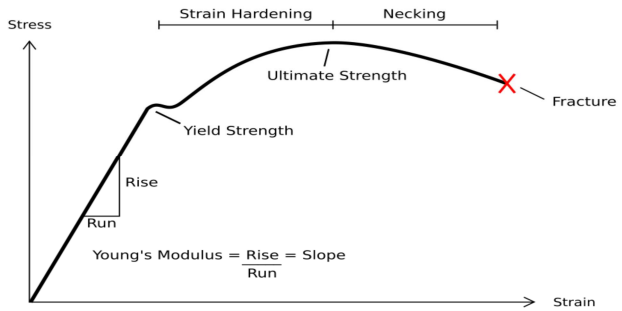

Figure 1. Plot of stress against strain for a typical structural steel [15].

There are various mathematical methods however based on different situations of the system. Mathematical methods that relates to materials that still obey hooks' law include finite strain theories, infinitesimal strain theories, plane strain theories, plane stress theories, beam theories and many more. Because of how complex each of these analyses may become, finite element analysis methodologies have been developed. Consequently countless software manufacturers have worked to produce FEA software's that can model the stress state of body under consideration and produce pictorial representations of same.

2.1. Finite Element Analysis (FEA) of a Connecting Rod

Modern engineering practices involves the use of sophisticated Computer Aided Designs (CAD) in solving complex problems with minimal errors, high level of accuracy and precision, less time etc. Such problems can involve mechanical components which come in different forms such as simple bars, beams connecting rod as well as complex systems like active suspension system of a dynamo bench which has multiple degrees of freedom. This FEA software comes in different commercial forms such as ANSYS, ADAMS, HYPERMESH, and CATIA etc. to mention but a few. In a typical mechanical member which is a continuous elastic structure (continuum), FEA irrespective of the geometry discretises the parts into small but finite well defined elements [11]. The FEA operates on a program that uses polynomial functions alongside matrix operations to help predict each discretised elements in relation to its material and geometric features where static loads or dynamic load can be applied within the defined nodal points [12]. However, these nodal points are the defining characteristics of any elements in the material. A node is composed of Degrees of Freedom (DOF) which is independent parameters that are used to ascertain the position of a particle in relation to its orientation in space. Depending on the complexity of the particle, the DOFs can be 1, 2, 3, or 6 as the case may be. If the elements within any mechanical member are defined locally in a matrix form, the elements are then assembled globally through their common DOFs into a complete system matrix. Having achieved this, determination of stresses and strains through constituting equations of elasticity becomes easier. In this case, the individual nodes that constitute the connecting rod will be discretised into fine mesh sizes and the stresses will be determined depending on the area of high stress concentration which is often denoted with red colour as well as other colours and their significance [1].

2.2. Plain Strain and Stress Theories

The 2D state of strain at any given point on the surface of a test

piece is defined by three independent variable which can either be (a) ε_x, ε_y, τ_{xy}; and (b) ε_1, ε_2, [5]. The assertion above is similar to what is obtainable for stresses also. From the aforementioned, Craig [5] observed that single resistance gauges measures unidirectional strains that have the same orientation with them. He however state that a direct method of measuring shear stresses along the x-y-plane is not possible with the use of single strain gauges. Engineers often use gauges at different positions on a test piece to be able to adequately analyse the stress situation of an irregular body under loading. If the strain in various directions is know it is possible using plane stress methods to compute the various stress states of a body. In the experiment, 3 strain gauges were placed at different points along the body of a connecting rod and two will have similar orientation and the other at 90 degrees to the others. The purpose of similar and different orientations is to ascertain that strain values is dependent on the orientation of the strain gauges. It is an often assumption that the principal strains (ε_1, ε_2) acts on the x and y-axes. The statement above therefore points out the fact that at any given time, computing the values of ε_1, ε_2, θ is important. Figure 2 shows the stress state of a body under system of forces;

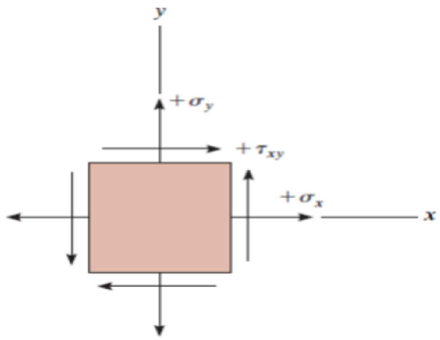

Figure 2. 2D Stress State of a body under system of loads.

For a body shown in Figure 2 above, the principal stresses are obtained by;

$$\sigma_{1,2} = \frac{\sigma_x + \sigma_y}{2} \pm \frac{1}{2}\sqrt{(\sigma_x - \sigma_y)^2 + \tau_{xy}{}^2} \quad (1)$$

Strain follows similar values and is given as;

$$\varepsilon_{1,2} = \frac{\varepsilon_x + \varepsilon_y}{2} \pm \frac{1}{2}\sqrt{(\varepsilon_x - \varepsilon_y)^2 + \gamma_{xy}{}^2} \quad (2)$$

However bodies under uniaxial loads obey Hooke's law in their elastic state. Such state is represented mathematically by general strain relations. The normal stress is given as;

$$\sigma = \frac{P}{A} \quad (3)$$

The normal strain is given as;

$$\varepsilon = \frac{\delta l}{L} \quad (4)$$

The Young modulus is given as;

$$E = \frac{\sigma}{\varepsilon} \quad (5)$$

And poison's ratio is given as;

$$\nu = \frac{\varepsilon_t}{\varepsilon_a} = \frac{\varepsilon_y}{\varepsilon_x} \quad (6)$$

Where

σ is the normal stress, τ is the shear stress, P is the load applied, A is the surface area perpendicular to the line of application of the forces, ε is the nominal strain, γ is the shear strain, δ is the change in length due to applied force, L is the original length of the test piece, $\nu$is the poisson ratio, ε_t is the lateral strain, ε_a is the longitudinal strain [6]

2.3. A Strain Gauges on the Connecting Rod

The use of the strain gauge on a connecting rod is due to proper optimization of this component when undergoing high cyclic loads which ranges from high compressive loads to high tensile loads in the combustion process due to the inertia [9]. It is aimed at achieving highest fuel efficiency of a vehicle. The connecting rod is a high volume production critical component which connects the reciprocating piston to the rotating crank shaft. Theconnecting rod is usually measured from centre to centre length which gives an influence on choice of material depending on the conditions of the engine. The compressive stresses have more influence due to the gas pressure because the gas pressure is the maximum load/force acting on the connecting rod which can be calculated experimentally and would be verified with the numerical calculation. Practically, the strain gauge used for the transfer steady state and transient data are mainly wire-less which is meant to meet the hostile environment conditions. These data's are transmitted through microwave and RF (radio frequency) transmission systems [7]. The connecting rods are majorly manufactured through either powdered metallurgy process or through forging from wrought steel. However, Young's Modulus is a very important property that contributes to the performance of the con rod during the in-service condition as it measures the stiffness of the connecting rod in order to determine how the connecting rod will stretch prior to breakage and it is a ratio of stress to strain. Figure 1 also show that by plotting a curve of stress against strain the resulting slope will always be the property called young's modulus of elasticity. The connecting rod which was quasi-statically loaded in tension, caused the material to elongate gradually against the applied load and the measured elongation which was recorded can be used in the calculation of engineering strain as shown in equation 7;

$$E = \frac{\Delta L}{L_o} = \frac{L - L_o}{L_o} = \frac{L}{L_o} - 1 \quad (7)$$

Where; ΔL is the change in gauge length

Lo is the initial gauge length and L is the final length.

3. Methodology

Experimental Procedures provided byVishay Precision Group [14] was adopted as the experimental procedures for the strain measurement. The basic idea in a tensile test is placing a material ofknown dimensions on the universal testing machine with one ends fixed while extending the other end until the material breaks at a point with the highest stress and strain concentration and tie rod is the material in this case. In this experiment, the resultant stresses along the connecting rod are caused by the strain which is a measure of the extent at which the connecting rod stretches (how much strain the connecting rod can undergo) when subjected to tensile loading. The idea was to measure the strain when the connecting rod is subjected to a tensile load and to compare the measured strains with those predicted by Finite Element Analysis.

3.1. Materials

Instron testing machine, Automotive connecting rod, Strain gauge(s), Strain gauge conditioning equipment, Strain gauge mounting kit, Soldering iron, Safety Glasses, PCT- 2M Gage Installation Tape.

3.2. Hand Calculations

The strain gauges are all situated on the shank of the connecting rod. However the location of the strain gauges is so close that it can easily be assumed that the gauges were located on the same line along the test piece. This means that an average value of readings from gauges 2 and 1 can be used in the analysis of results. The cross section of the connecting rod at the point of application of the strain gauges is shown in Figure 3. The third gauge is perpendicular to the axes of the applied force and hence measures compressive strain rather than the tensile strain measured by both gauges 1 and 2.

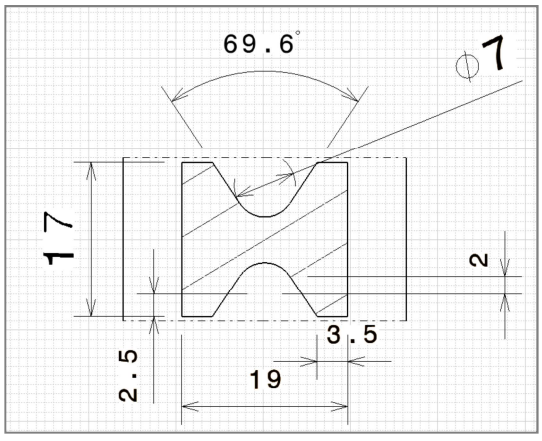

Figure 3. Rough sketch of the cross section of the measurement area.

From Figure 3, the cross sectional area was obtained as 243.17 mm^2. However because of the difficulty in locating the probe at an exact point, the location of gauge 2 was used and therefore the readings for gauge 2 were used for the calculations as follows. Recall that the stress at a point is a ratio of force and cross sectional area. We can therefore obtain the nominal stress by using equation 3

$$(\sigma = \frac{P}{A}).$$

For F = 475 N,

$$\sigma = \frac{475}{243.17} = 1.9534\ MPa$$

The young's modulus is given by equation 5 as$E = \frac{\sigma}{\varepsilon}$

$$E = \frac{1.953365957971789}{13\mu} = 150.26\ GPa$$

To calculate poison's ratio, the strain on the x-axis is compared to that on the y or z axis as the case may be. For the first load case,

$$\nu = \left|\frac{\varepsilon_1}{\varepsilon_2}\right| = \left|\frac{0}{17}\right| = 0$$

The computed results for both stress and young's modulus are shown in Table 1.

Table 1. Results of Stress calculations.

Force (N)	$\varepsilon_{1(\mu)}$	$\varepsilon_{2(\mu)}$	$\varepsilon_{3(\mu)}$	Average $\varepsilon_{1(\mu)}$	Stress (MPa)	E (GPa)	ν
475	0	13	17	15.0	1.9534	150.26	0.033
1028	-1	30	37	33.5	4.2275	140.92	0.080
1680	-4	50	61	55.5	6.9087	138.17	0.159
2260	-11	69	82	75.5	9.2939	134.69	0.193
2823	-17	88	104	96.0	11.6092	131.92	0.225
3492	-25	111	129	120.0	14.3603	129.37	0.240
3900	-30	125	145	135.0	16.0382	128.31	0.257
4600	-38	148	170	159.0	18.9168	127.82	0.033

To model the experimental setup in FEA software, the test piece was constraint to be fixed at the smaller hole of the con rod and loaded at the larger end. A major determinant of results from FEA is the mesh size. It is often necessary to optimize between results and the processing time for any analysis. To be able to check what point the results will converge, the analysis was done with different mesh sizes. Figure 4 shows different mesh sizes for the test piece. The results of the simulation from CATIA and ANSYS for the same test piece were compared and 10mm mesh size showed results that were a little wide from each other considering the von-mises result. With ANSYS giving a higher result, it would be safer to use the higher result to ensure conformity

in all instances. Comparing the results of the simulation for mesh sizes 10 mm, 5 mm and 3 mm, it can be observed that there is a relative increase between 10 mm mesh and 5 mm mesh and in both CATIA and ANSYS these results differed. For 3 mm mesh size, the results obtained for the two FEA software had negligible difference.

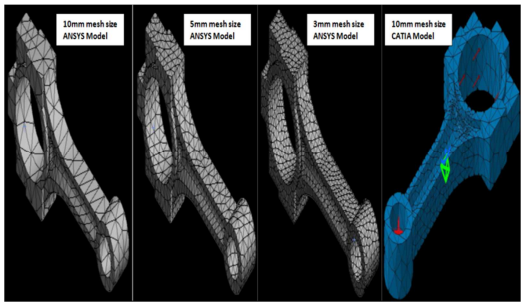

Figure 4. ANSYS Model for 10mm, 5mm and 3mm mesh size and CATIA Model for 10mm mesh size.

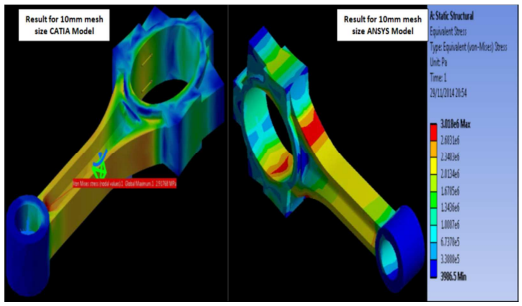

Figure 5. CATIA Result with 10 mm mesh size and ANSYS Result with 10 mm mesh size of the same test piece.

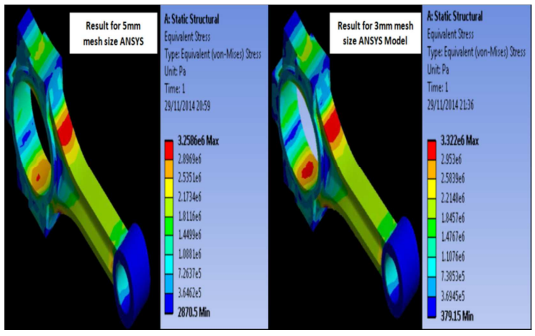

Figure 6. ANSYS Result with 5 mm mesh size and ANSYS Result with 3 mm mesh size of the same test piece.

To compile the results, the 3 mm mesh size was therefore used. The results of the simulation for the other mesh sizes are produced in Figures 6 above. The result shows the von-mises stress for the setup to be around 3.322 Mpa at a force of 475 N. To compute the factor of safety the von-mises stress is compared to the yield strength of the material as follows;

$$\text{Factor of Safety} = \frac{\text{Yield Strength}}{\text{Allowable Stress or Von-mises}} \quad (8)$$

For a 475 N force, the von-mises stress is 3.322 Mpa while the yield strength of steel is 250 MPa. The Factor of safety is therefore;

$$\text{Factor of Safety} = \frac{250}{3.322} = 75.26$$

Presented in Table 2, are the maximum value of the stresses and the subsequent factor of safety for each load case. At about a force between 18 KN and 20 KN, the simulation shows that if the body is given a factor of safety of 2.0, the connecting rod will fail. The factor of safety is however necessary in mechanical engineering designs because users of engineering products often times overload engineering products above designed limit a low Factor of Safety (F.O.S) means that with a little additional load, the material will exceed its elastic region and result in a permanent deformation.

Table 2. Computed factor of safety for each load case.

Force (N)	Min Von-mises Stress (MPa)	Min Von-mises Stress (MPa)	Factor of Safety
475	0.0003792	3.322	75.2559
1028	0.0008206	7.190	34.7724
1680	0.0013410	11.750	21.2766
2260	0.0018039	15.806	15.8168
2823	0.0022533	19.743	12.6627
3492	0.0027873	24.422	10.2367
3900	0.0031130	27.276	9.1656
4600	0.0036717	32.171	7.7710

Because of the inaccuracy of locating the position of the gauges, a strain and stress probe was positioned at point -62.83, 9.50, -0.038 corresponding to 62.83 mm from the smaller end of the connecting rod and on the surface of the shank as positioned in the experiment. Figure 7 shows the position of the probe and the results of the strain probe are tabulated in Table 3. This values will however be compared with the experimental results.

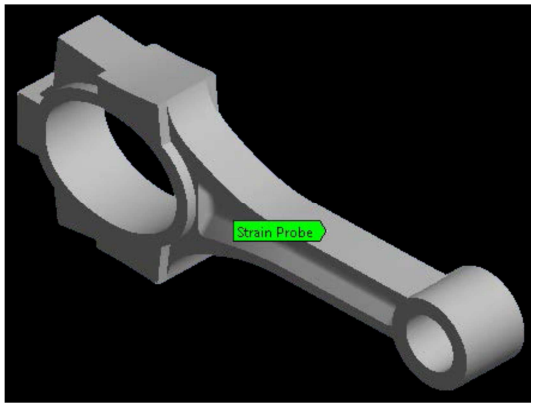

Figure 7. Connecting rod CAD model with strain probe location.

The results shown in Table 3 includes the principal strains, the strain intensity, the nominal strains and the shear strain values, while the results shown inTable 4 also includes the stress intensity, the principal, the nominal and the shear stress values.

Table 3. ANSYS Result of strain probe.

Strain Values from Probe (μ)										
Normal Strain			Shear Strain			Equivalent	Principal Strain			
X	Y	Z	XY	YZ	XZ	Von-mises	Max	Middle	Min	Intensity
10.09	-2.91	-3.33	0.06	-0.01	0.01	10.17	10.09	-2.91	-3.33	13.43
21.84	-6.29	-7.21	0.13	-0.02	0.03	22.01	21.84	-6.29	-7.21	29.06
35.70	-10.28	-11.78	0.22	-0.03	0.05	35.97	35.70	-10.28	-11.78	47.48
48.02	-13.83	-15.85	0.30	-0.04	0.06	48.38	48.02	-13.83	-15.85	63.88
59.99	-17.28	-19.80	0.37	-0.04	0.08	60.44	59.99	-17.28	-19.80	79.79
74.20	-21.37	-24.49	0.46	-0.05	0.10	74.76	74.20	-21.37	-24.49	98.70
82.87	-23.87	-27.36	0.51	-0.06	0.11	83.49	82.87	-23.87	-27.36	110.23
97.75	-28.15	-32.27	0.60	-0.07	0.13	98.48	97.75	-28.15	-32.27	130.01

Table 4. ANSYS Result of stress probe.

Stress Values from Probe (MPa)										
Normal Stress			Shear Stress			Equivalent	Principal Stress			
X	Y	Z	XY	YZ	XZ	Von-mises	Max	Middle	Min	Intensity
2.00	0.00	-0.07	0.00	0.00	0.00	2.03	2.00	0.00	-0.07	2.07
4.32	-0.01	-0.15	0.01	0.00	0.00	4.40	4.32	-0.01	-0.15	4.47
7.07	-0.01	-0.24	0.02	0.00	0.00	7.19	7.07	-0.01	-0.24	7.31
9.50	-0.01	-0.32	0.02	0.00	0.00	9.68	9.50	-0.01	-0.32	9.83
11.87	-0.01	-0.40	0.03	0.00	0.01	12.09	11.87	-0.01	-0.40	12.28
14.69	-0.02	-0.50	0.04	0.00	0.01	14.95	14.69	-0.02	-0.50	15.18
16.40	-0.02	-0.56	0.04	0.00	0.01	16.70	16.40	-0.02	-0.56	16.96
19.35	-0.02	-0.66	0.05	-0.01	0.01	19.69	19.35	-0.02	-0.66	20.00

4. Discussion of Results

A few components of the result necessary in this experiment is given in Table 5. A descriptive analysis of the important parameters obtained from measurement and FEA is also presented in the Table 6.

Table 5. Stress Strain results for different Load cases.

Force (N)	$\varepsilon_{1(\mu)}$	$\varepsilon_{2(\mu)}$	Stress (MPa)	F.O.S	Strain Intensity (μ)	Stress Intensity (μ)	Z (μ)
475	0	13	1.9534	75.2559	13.43	2.07	-3.33
1028	-1	30	4.2275	34.7724	29.06	4.47	-7.21
1680	-4	50	6.9087	21.2766	47.48	7.31	-11.78
2260	-11	69	9.2939	15.8168	63.88	9.83	-15.85
2823	-17	88	11.6092	12.6627	79.79	12.28	-19.8
3492	-25	111	14.3603	10.2367	98.7	15.18	-24.49
3900	-30	125	16.0382	9.1656	110.23	16.96	-27.36
4600	-38	148	18.9168	7.771	130.01	20.00	-32.27

Table 6. Descriptive analysis of Stress Strain parameters for different Load cases.

	Force (N)	$\varepsilon_{1(\mu)}$	$\varepsilon_{2(\mu)}$	Stress (MPa)	F.O.S	Strain Intensity (μ)	Stress Intensity (μ)	Z (μ)
Mean	2532.25	-15.75	79.25	10.41	23.37	71.57	11.01	-17.76
Standard Error	507.93	5.02	16.73	2.09	8.04	14.36	2.21	3.56
Median	2541.50	-14.00	78.50	10.45	14.24	71.84	11.06	-17.83
Mode	#N/A	#N/A	#N/A	#N/A	#N/A	#N/A	#N/A	#N/A
Standard Deviation	1436.64	14.20	47.33	5.91	22.73	40.60	6.25	10.08
Sample Variance	2063925.93	201.64	2239.93	34.90	516.55	1648.61	39.00	101.58
Kurtosis	-1.18	-1.34	-1.23	-1.18	4.62	-1.18	-1.18	-1.18
Skewness	-0.03	-0.39	0.03	-0.03	2.12	-0.03	-0.03	0.03
Range	4125.00	38.00	135.00	16.96	67.48	116.58	17.93	28.94
Minimum	475.00	-38.00	13.00	1.95	7.77	13.43	2.07	-32.27
Maximum	4600.00	0.00	148.00	18.92	75.26	130.01	20.00	-3.33
Sum	20258.0	-126.0	634.00	83.31	186.96	572.58	88.10	-142.09
Count	8.00	8.00	8.00	8.00	8.00	8.00	8.00	8.00
Confidence Level (95.0%)	1201.06	11.87	39.57	4.94	19.00	33.95	5.22	8.43

As expected, the strain probe results show that the normal stress in the X-direction is equal to the maximum stress while the minimum principal strain equals that on the z-axis. This confirms that the measurement as asserted before, the values obtained from the strain gauges 2 and 3 correspond to the principal strain as the measurement is taken in the principal axis of the acting force. This confirms that the FEA results can be accepted. To further justify the acceptance of the FEA result, a correlation of the results for strain and stress were carried out. The strain intensity from the probe was compared to the result obtained from strain gauge 2. The correlation returned a value of 0.999775796. This implies that the values obtained are closely related. The procedure was repeated for stress values and it returned a correlation value of 0.999999806. With these values, the FEA result can therefore be accepted to represent closely the actual situation of the static load on the connecting rod.

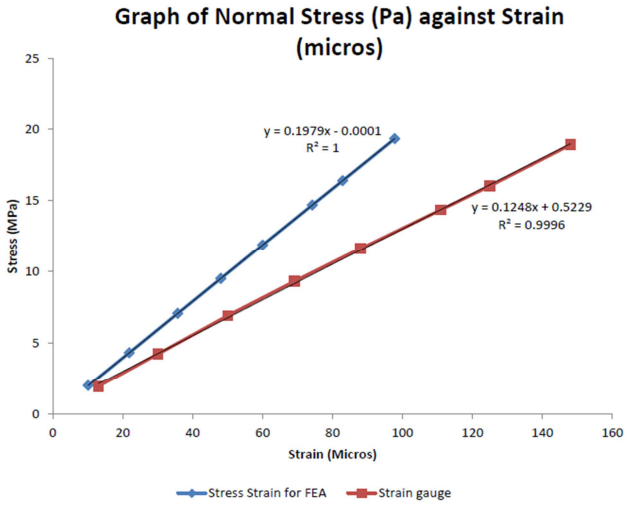

Figure 8. Plot of Axial Stress against Strain.

The graph of stress against strain is plotted as shown in Figure 8 above. The plot compares the result for strain gauge 2 and the computed stress against that of stress and strain obtained in FEA software. The result for the FEA software gave a slope of 197.9 Gpa while that of the measurement gave a slope of 124.8 Mpa. This is expected because the stress pattern in the connecting rod will vary as a result of variation in surface area. This implies that a simple calculation of normal stress will not be enough to evaluate the stress at any point in a solid with variation in its surface area from point to point. This observation is enough to justify the essence of a complex analysis of bodies under loading using Finite Element analysis. Table 7 provides a descriptive summary of the load and elongations recorded during the experiment. These values are subsequently used to plot a load extension graph the slope of which represents the stiffness of the connecting rod. The load-extension graph is presented in Figure 9. The mean extension stands at 0.2511 mm while the force has a mean value of 1944. The load-extension graph gave a slope of 13.3 MN/m. This represents the stiffness of the whole system.

Table 7. Descriptive Summary of the Load and Elongations.

	Extension	Force
Mean	0.251103	1944.969
Standard Error	0.002076	28.04583
Median	0.25951	1953.387
Mode	0.13246	364.2678
Standard Deviation	0.083697	1130.563
Sample Variance	0.007005	1278174
Kurtosis	-0.39738	-1.19882
Skewness	-0.45651	-00678
Range	0.38166	3912.038
Minimum	0.00043	-6.71744
Maximum	0.38209	3905.32
Sum	408.0431	3160575
Count	1625	1625
Confidence Level (95.0%)	0.004072	55.00981

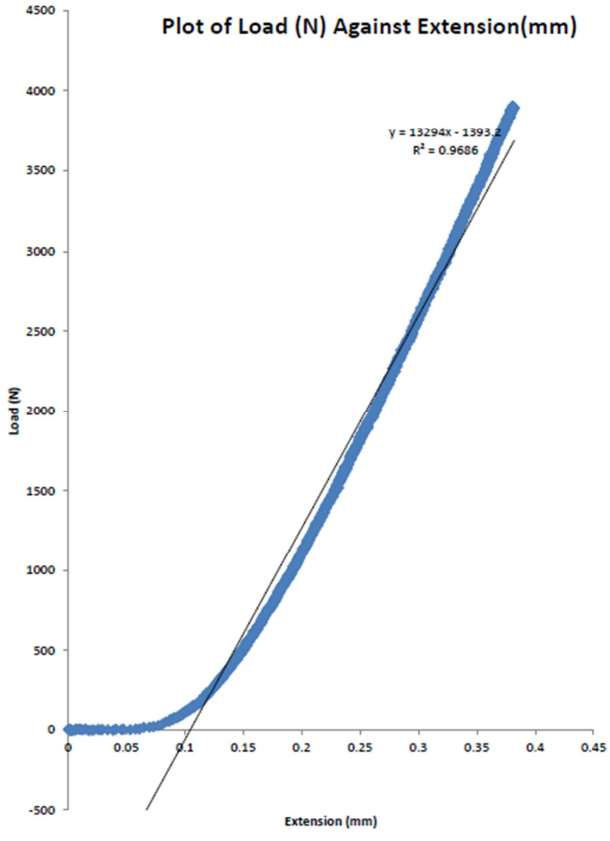

Figure 9. Plot of Axial Load against Extension.

4.1. Possible Sources of Error

Various discrepancies in the results presented in this report may be due to technical error in

i. Setup of the experiment

ii. Measuring Instruments

iii. FEA Model

4.2. Experimental Errors

Sources of errors in the experimental setup may include:

i. Stress concentration as a result of surface preparation defects.

ii. Low sensitivity to the measuring surface as a consequence of high quantity of bonding agent

iii. Improper clamping of the test piece

4.3. Possible Sources of Error in the Experiment

i. Linearity-Pressure changes may change the sensitivity of the gauge.

ii. Hysteresis. This means the gauge does not return to zero after load is withdrawn

iii. Repeatability.

iv. EMI induced errors

v. Zero Offset-this kind of error may be introduced during bonding of the strain gauge. Temperature coefficient of Gauge Factor (TCGF)-This is the change of sensitivity of the device to strain with change in temperature.

vi. Zero Shift with temperature-If the TCGF of each gauge is not the same, there will be a zero shift with temperature. This is also caused by anomalies in the force collector. This is usually compensated for with one or more resistors strategically placed in the compensation network.

vii. Overloading

viii. Humidity: corrosion can make current flow to the test piece from the gauge if it is not prevented against humidity. This may alter the result of the experiment.

4.4. FEA Errors

By constraining the test model wrongly, the FEA may produce values that are different from expected results. If wrong material properties are applied, this can also result in wrong results. The mesh size used can also affect the result of the analysis. Other factors that affect results are as follows:

i. HUMAN ERRORS requires inputs before it can run, as errors are bound to occur as it is

ii. The input parameters are obtained as the output. In other words, if the input is incorrect, then the result obtained will be incorrect as well.

iii. It utilizes a general closed form solution.

iv. It obtains approximate solutions.

v. It contains inherent errors as well.

5. Conclusion

By comparing the results of strain and stress obtained from FEA analysis and measurement taken for strain in the lab with strain gauges, it is easy to conclude that FEA will be an adequate tool for static analysis of structures. The results obtained from each procedure shows close relationship which implies that FEA analysis is viable and can be recommended. Notwithstanding, the closeness of values obtained, FEA analysis could become very cumbersome and require a lot of processing time. It is therefore necessary that an agreement between accuracy of results and processing time be used in guiding to determine which mesh size is best utilized in the analysis. This may however vary for each case in consideration. It is also important that in engineering designs, factor of safety be taken into consideration to be able to help guaranty the safety of the equipment under use.

References

[1] Budynas, G. and Nisbett, J. (2008) Shigley's Mechanical Engineering Design. 8th Edition in SI Units. Publisher: McGraw-Hill Company Inc, New York. ISSN: 9780071268967.

[2] Business Dictionary (2014) *What is Hooke's Law? definition and meaning.* [Online] Available from <http://www.businessdictionary.com/definition/Hooke-s-Law.html> [25 September 2015].

[3] Boresi, A. P., Schmidt, R. J. and Sidebottom, O. M. (1993) Advance Mechanics of Materials, Wiley.

[4] Brannon, R. (2012) Distinction between Uniaxial Stress and Uniaxial Strain. University of Utah Computational Solid Mechanics Research Group, University of Utah.

[5] Craig, J. I. (2013) *Strain Transformation and Rosette Gage Theory.* [online] available from <http://soliton.ae.gatech.edu/people/jcraig/classes/ae3145/Lab2/strain-gage-rosette-theory.pdf> [1 August 2015].

[6] Dan, M. B., Christian, D. I. and Bogdan, C. O. (2001) Mechanics of Material.5th ed. USA: Academic Press.

[7] Dasar, E. (2013) *Sensor Strain Gauge.* [online] available from <http://elektronika-dasar.web.id/komponen/sensor-tranducer/sensor-strain-gauge/> [30 October 2014].

[8] Ferdinand, B. P., Russell, J. E., John, D. T. and David, M. F. (2010) Mechanics of Material. New York: McGraw Hill Companies.

[9] Jim, M. (2010) *Connecting Rods - Enginology.* [online] Available from <http://www.hotrod.com/how-to/engine/ctrp-1011-connecting-rods/> [22 September 2014].

[10] Lanza, G. (1885) *Applied mechanics. Publishers:* J Willey & Sons, New York.

[11] Qinghui, Z., Yunying, W. and Wei, J. (2010) The Finite Element Analysis of Connecting Rod of Diesel Engine. Published in international Conference on Measuring Technology and Mechatronics Automation on13-14 March 2010, 3, 870-873. ISBN: 978-1-4244-5001-5, IEEE.

[12] Shenoy, P. S. (2004) Dynamic Load Analysis and Optimization of Connecting Rod. Department of Mechanical Engineering, University of Toledo.

[13] Slaughter, W. S. (2001) The Linearized Theory of Elasticity, Birkhauser. ISBN: 9780817641177.

[14] Vishay Precision Group (2010) Strain Gage Installations with M-Bond 200 Adhesive, Toronto: Inter-technology Inc.

[15] Wikimedia (2008) *Stress Strain Ductile Material.png-Wikimedia Commons.* [online] available from <http://commons.wikimedia.org/wiki/File:Stress_Strain_Ductile_Material.png> [20 September 2014].